

CHAPTER 2

ACCELERATOR PHYSICS FUNDAMENTALS

This chapter describes the coordinate systems and magnet strength definitions used in the remainder of this thesis. Because a thorough background in accelerator physics is not assumed and definitions used by various researchers within the field typically vary, aspects of the field are also discussed here that are relevant to the remainder of this work. In § 2.1 the local transverse coordinate system used to expand transverse motion in a synchrotron is described, as well as the definitions of both linear and nonlinear magnet strengths. In § 2.2 the transverse linear dynamics of a strong-focusing synchrotron are discussed. In § 2.3 the discrete Hamiltonian formalism that will be used to investigate the nonlinear dynamics of this system is introduced, and the forms of generating functions and transformations that will be applied to the discrete Hamiltonian in Chapters 3 and 4 are described; § 2.4 returns to investigate the longitudinal motion in a synchrotron and how this motion couples to the transverse dimension.

Table (2.1) lists typical values of many quantities relevant to accelerator operations at the Tevatron collider, the Indiana University Cyclotron Facility (IUCF) cooling ring and the SSC collider. Many of these quantities are not mentioned here in detail, but are listed for completeness.

2.1 ACCELERATOR COORDINATE SYSTEMS

Typically the equilibrium orbit, or closed orbit, around a synchrotron can be approximated as a circle with a constant radius ρ — this is equivalent to stating that the accelerator approximately consists of nothing but dipole magnets, ignoring the effects of vertical bends and long straight sections. (For example, 75% of the Fermilab Tevatron and 80% of the Fermilab Booster circumferences consist

Parameter	Symbol (units)	FNAL TeV	IUCF Cooler	SSC Collider
Horizontal Tune	Q_x	20.586	3.82	123.28
Vertical Tune	Q_y	20.575	4.85	123.78
Synchrotron Tune	Q_s	$5.7 \cdot 10^{-4}$	$5 \cdot 10^{-4}$	$1.2 \cdot 10^{-3}$
Revolution Freq.	f_{rev} (kHz)	47.7	10^3	3.4
Minimum Beta	β^* (m)	0.5	1	1
Maximum Beta	β_{max} (m)	200	50	$8 \cdot 10^3$
Dispersion (ave.)	η (m)	0.5	0.2	1
Momentum Spread	σ_p/p	$2 \cdot 10^{-4}$	$4 \cdot 10^{-5}$	10^{-4}
Kinetic Energy	E (GeV)	900	0.045	$2 \cdot 10^4$
Rigidity	$ B\rho $ (T-m)	$3 \cdot 10^3$	3.6	$7 \cdot 10^4$
Bend Radius	ρ (m)	$7.5 \cdot 10^2$	1.2	$1.0 \cdot 10^4$

Table 2.1: Various operational accelerator parameters for the Fermilab Tevatron collider (1993 collider lattice), the IUCF cooling storage ring and the SSC collider (Design Report). For the colliders the values given refer to a single beam.

of dipole magnets.) All transverse motion is expanded in the transverse displacements from this equilibrium closed orbit, with \hat{x} being defined in the outward radial direction. The direction of beam travel on the closed orbit is defined as \hat{s} , always tangential to the closed orbit; then $\hat{y} \equiv -\hat{x} \times \hat{s}$ and the triplet $(\hat{x}, \hat{y}, \hat{s})$ forms a right-handed coordinate system. This agrees with the convention used in the MAD 8.1 and TEAPOT lattice design and tracking programs (Grote and Iselin 1990, Schachinger and Talman 1985), as well as that of Edwards and Syphers (Edwards and Syphers 1987).

In such a coordinate system, the magnetic dipole bending field \vec{B}_0 for a positively charged particle is oriented in the $+\hat{y}$ direction; this makes it natural to speak of a field error as being positive if it points in this direction. For a typical proton synchrotron with normal temperature dipoles this magnetic field can be as high as 2 Tesla; with superconducting dipoles such as those used in RHIC, the

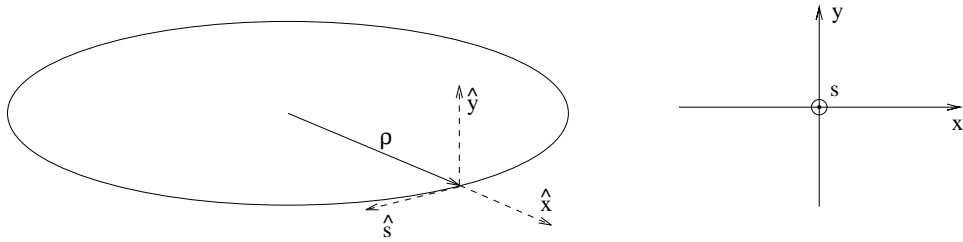


Figure 2.1: The local coordinate system in a synchrotron.

CERN LHC, the Tevatron and the SSC, B_0 can be as high as 6.6 Tesla. Magnetic fields and field errors can now be analytically expanded by

$$i\Delta B_x + \Delta B_y = B_0 \sum_{n=0}^{\infty} (b_n + ia_n)(x + iy)^n, \quad (2.1)$$

where the b_n denote multipole strengths of normal field components and the a_n denote multipole skew field components. The units of these multipole strengths are m^{-n} , and the strengths themselves range from $.3 m^{-2}$ for sextupole correctors in the Tevatron to approximately $10^{-4} m^{-n}$ for higher order multipole errors from fringe fields or magnet coil misalignments.

This field expansion agrees with the multipole strength conventions used in TEAPOT, but does not agree with the conventions used by MAD 8.1, which instead uses a Taylor expansion for the magnetic field on the midplane of the magnet, $y = 0$. A comparison of the two definitions for normal multipole strengths gives the relationship

$$b_n(\text{thesis}) = b_n(\text{TEAPOT}) = \frac{B_n(\text{MAD})}{n!B_0} = \frac{1}{n!B_0} \left(\frac{\partial^n B_y}{\partial x^n} \right)_{y=0}. \quad (2.2)$$

Typically magnetic multipole strengths are measured from angular fourier analysis of field strengths for a distribution of angular positions at a constant radius from the magnet center bore.

In this dissertation we make the normally realistic approximation that kicks from nonlinear magnetic fields are small and applied over a negligible magnet

length L , or that the transverse momentum change from the nonlinearity is small compared to the total momentum of the kicked particle. The following discussion is therefore only relevant for kicks applied over short distances such as those from dipole fringe fields, quadrupoles and correctors; it does not trivially apply to multipole errors within long dipoles. The small-amplitude kicks over a short multipole are given by

$$\Delta x' = -\frac{L}{|B\rho|}\Delta B_y, \quad \Delta y' = \frac{L}{|B\rho|}\Delta B_x. \quad (2.3)$$

Here $|B\rho|$ is the magnetic rigidity, related to the particle's total momentum p and charge e by $|B\rho| = p/e$; units are such that $|B\rho| \approx 3.3357pc$ for a particle with electron or proton charge when pc is expressed in GeV and $B\rho$ in T-m. The prime denotes differentiation with respect to the longitudinal coordinate s , so $x' \equiv dx/ds$. We then have

$$\Delta x' - i\Delta y' = -\frac{B_0 L}{|B\rho|} \sum_{n=0}^{\infty} (b_n + ia_n)(x + iy)^n. \quad (2.4)$$

For the $n = 0$ case (the primary dipole bending field) $b_0 = 1$ in the horizontal plane and the quantity $B_0 L/|B\rho|$ is the bend angle for each main dipole.

In the case of a normal quadrupole, for example, $n = 1$ and

$$\Delta x' - i\Delta y' = -\frac{B_0 L}{|B\rho|} b_1 (x + iy). \quad (2.5)$$

For a positive normal quadrupole strength b_1 a particle displaced positively in the \hat{x} direction receives a negative (focusing) kick. In the \hat{y} direction, however, a positively displaced particle is given a positive (defocusing) kick.

In this thesis dispersive effects are ignored except for a few comments about sources of beta modulation in Chapter 4 — particle energies are held constant and there is no variation in the rigidity $|B\rho|$ which affects relative field strengths. For simplicity in the notation we therefore absorb the leading term (the dipole bend

angle) into the multipole strength terms and rewrite the multipole kick expansion (2.4) as

$$\Delta x' - i\Delta y' = - \sum_{n=1}^{\infty} (\tilde{b}_n + i\tilde{a}_n)(x + iy)^n, \quad (2.6)$$

where $(\tilde{b}, \tilde{a})_n \equiv (b, a)_n B_0 L / |B\rho|$. These are called the normalized multipole strengths and have the units m^{-n} .

2.2 TRANSVERSE LINEAR MOTION IN A SYNCHROTRON

By far the most influential paper in accelerator physics has been that of Courant and Snyder (1958), which laid the foundations for much of the field. There the transverse linear motion near the closed orbit of an alternating-gradient synchrotron was shown to be parameterized by a pair of quantities, $\beta(s)$ and $\alpha(s) \equiv -\beta'(s)/2$, for each transverse plane of oscillation. With the dispersion function $\eta(s)$ (see Equation (2.33)) these parameters are commonly referred to as the lattice functions of the accelerator.

The “beta function” $\beta(s)$ has units of length — it ranges from approximately half a meter to 200 meters in the Tevatron collider lattice. As will be shown shortly, the amplitude of transverse particle oscillations scales with $\sqrt{\beta(s)}$ in motion around the accelerator. At the interaction regions of many colliders, a low-beta insertion is designed to lower the beta function at the beam crossing point, thus reducing the actual beam size and increasing the luminosity.

Motion of particles in the two transverse planes is coupled even in the linear approximation by a variety of perturbations such as longitudinal solenoidal fields from experimental detectors, normal dipole and quadrupole rotation errors, vertical dipole bends and deliberately installed skew quadrupoles. With the assumption that the accelerator under consideration is flat and that there are no significant solenoidal fields, this coupling is usually small and treated perturba-

tively. Such a treatment is followed in this thesis, and allows the linear motion in each of the transverse planes to be treated as independent.

In either transverse dimension the motion of a particle through the straight drift sections, dipoles and quadrupoles of a synchrotron is described by Hill's equation,

$$x''(s) + K(s)x(s) = 0 , \quad (2.7)$$

where $K(s)$ the focusing strength in that plane, piecewise continuous and periodic over one revolution of the machine. If the synchrotron has a superperiodicity, $K(s)$ naturally also has this superperiodicity — however, this symmetry is normally broken by low-beta insertions or other practical necessities.

Because Hill's equation is so similar to the equation of motion of a harmonic oscillator, it is typically solved by substituting a harmonic solution where both the amplitude and phase depend on s :

$$\begin{aligned} x(s) &= \sqrt{2J\beta(s)} \cos \psi(s) \\ &= a(s) \cos \psi(s) . \end{aligned} \quad (2.8)$$

The choice of normalization here is motivated by transformations derived in the next section, where J is shown to be the action canonical to the phase $\psi(s)$. Substitution of this ansatz into Equation (2.7) gives two differential relations for $\psi(s)$ and $\beta(s)$:

$$\frac{d}{ds}(\beta\psi') = 0 , \quad (2.9)$$

$$2\beta''\beta - (\beta')^2 - 4\beta^2(\psi')^2 + 4\beta^2K(s) = 0 . \quad (2.10)$$

Equation (2.9) can be integrated immediately, using the standard convention that chooses the constant of integration as one, to find the integrated phase,

$$\psi(s) = \int_0^s \frac{dS}{\beta(S)} . \quad (2.11)$$

Similarly the phase advance over any section of the ring (s_1, s_2) can be defined:

$$\Delta\psi = \int_{s_1}^{s_2} \frac{dS}{\beta(S)}. \quad (2.12)$$

With this ψ' , Equation (2.10) for the betatron function $\beta(s)$ takes the standard forms:

$$\begin{aligned} 2\beta''\beta - (\beta')^2 + 4\beta^2 K(s) &= 4, \\ 1 + \alpha'\beta + \alpha^2 &= \beta^2 K(s). \end{aligned} \quad (2.13)$$

With periodic boundary conditions and piecewise continuous $K(s)$ this equation can be solved numerically to give the betatron function β as a function of s .

The tune Q in each plane is defined as the long-term average number of transverse betatron oscillations executed in that plane in each traversal of the ring, or the average transverse oscillation frequency divided by the revolution frequency of the machine. It is found in the linear approximation by taking the total phase advance over one traversal and dividing by 2π :

$$Q \equiv \frac{1}{2\pi} \oint dS/\beta(S). \quad (2.14)$$

Generally the solution to any linear second-order differential equation such as Equation (2.7) is uniquely determined by the initial conditions of x and x' . It has been shown (Courant and Snyder 1958) that the linear motion in each plane over any section (s_1, s_2) of the ring can be completely described by

$$\begin{pmatrix} x \\ x' \end{pmatrix}_2 = M_{21} \begin{pmatrix} x \\ x' \end{pmatrix}_1, \quad (2.15)$$

where

$$M_{21} = \begin{pmatrix} \sqrt{\frac{\beta_2}{\beta_1}}(\cos \Delta\psi + \alpha_1 \sin \Delta\psi) & \sqrt{\beta_1\beta_2} \sin \Delta\psi \\ \frac{-(1+\alpha_1\alpha_2) \sin \Delta\psi - (\alpha_2 - \alpha_1) \cos \Delta\psi}{\sqrt{\beta_1\beta_2}} & \sqrt{\frac{\beta_1}{\beta_2}}(\cos \Delta\psi - \alpha_2 \sin \Delta\psi) \end{pmatrix}. \quad (2.16)$$

The same mapping also holds for motion in the y plane, using lattice functions and phase advances there. The linear transformation matrix M_{21} is a combination

of rotations and scalings which map the particles around a rotation on an ellipse in the phase space (x, x') ; it is unwieldy in this basis because the parameters β and ψ are more natural for a circular coordinate system as will be shown in the next section.

The transformation matrix M_{21} is actually a concatenation of several individual transformation matrices which can be found by solving simpler versions of Hill's equation. For the case where K is zero, as is true in straight drift sections and approximately true in dipoles of length L ,

$$M_{21}(K = 0) = \begin{pmatrix} 1 & L \\ 0 & 1 \end{pmatrix}. \quad (2.17)$$

For the case where K is a nonzero constant, as in a quadrupole of length L ,

$$M_{21}(K = \text{constant}) = \begin{pmatrix} \cos(L\sqrt{K}) & \frac{1}{\sqrt{K}}\sin(L\sqrt{K}) \\ -\sqrt{K}\sin(L\sqrt{K}) & \cos(L\sqrt{K}) \end{pmatrix}. \quad (2.18)$$

Keeping the integrated magnet strength $KL = \tilde{b}_1$ constant while taking the thin magnet limit $L \rightarrow 0$ here gives the transformation matrix of a thin horizontal quadrupole kick,

$$M_{21}(\text{thin quad}) = \begin{pmatrix} 1 & 0 \\ -\tilde{b}_1 & 1 \end{pmatrix}. \quad (2.19)$$

Since a horizontally focusing quadrupole defocuses equally in the vertical direction (see Equation (2.5)), reversing the sign of \tilde{b}_1 in the above mapping gives the corresponding thin quadrupole kick in the vertical plane.

For the subjects examined in this dissertation, motion is only observed once per accelerator turn in a Poincaré surface of section; in this approach, the transverse phase space is observed in discrete time steps instead of continuously around the ring. This method of visualization is more practical in application, because beam position monitors and other diagnostic equipment measure beam properties on a turn-by-turn basis. The longitudinal coordinate s is transformed to an integer

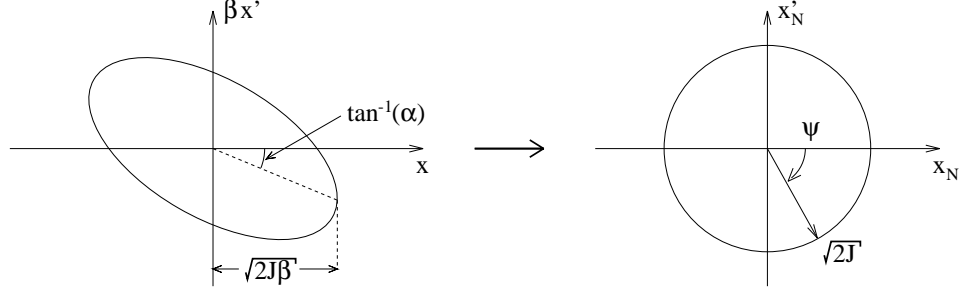


Figure 2.2: The phase space ellipse transformation (2.23) from physical transverse coordinates (x, x') to normalized transverse coordinates (x_N, x'_N) . The physical amplitude of betatron oscillations at a point with beta function β is $a = \sqrt{2J\beta}$.

turn-number coordinate $t \equiv [s/2\pi\rho]$ so the mapping represented by Equations (2.15) and (2.16) now becomes a “one-turn map”:

$$\begin{pmatrix} x \\ x' \end{pmatrix}_{t+1} = M \begin{pmatrix} x \\ x' \end{pmatrix}_t, \quad (2.20)$$

where the linear one-turn transformation matrix is

$$M = \begin{pmatrix} \cos(2\pi Q) + \alpha \sin(2\pi Q) & \beta \sin(2\pi Q) \\ -\frac{(1+\alpha^2)}{\beta} \sin(2\pi Q) & \cos(2\pi Q) - \alpha \sin(2\pi Q) \end{pmatrix} \quad (2.21)$$

and the lattice functions β and α are those of the observation point. It is also interesting to note that imposing a small thin quadrupole kick on the one-turn map gives the tune shift associated with a quadrupole error of strength \tilde{b}_1 as

$$\Delta Q_{x,y}(\text{quad}) = \pm \frac{\tilde{b}_1 \beta(\text{quad})}{4\pi}, \quad (2.22)$$

with the positive sign referring to the horizontal plane and the negative to the vertical.

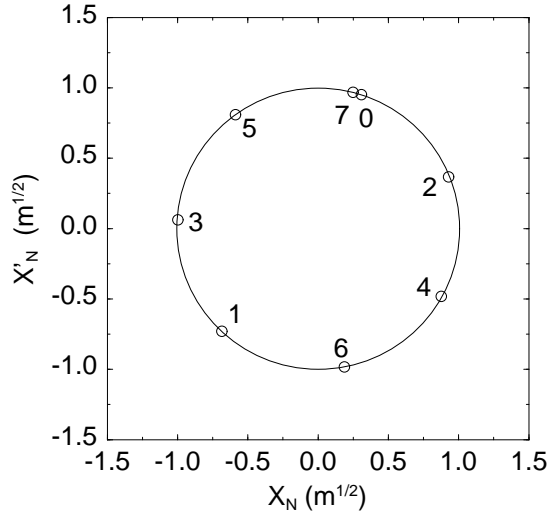


Figure 2.3: Seven turns of a linear one-dimensional turn-by-turn Poincaré plot in normalized coordinates (x_N, x'_N) , with tune $Q = .57$ near the $4Q = 7$ resonance. This is simulation of a single particle following the linear one-turn map of Equation (2.20); each successive point lies on a circular contour.

A coordinate transformation exists that transforms the elliptical mapping of Equation (2.21) into a circular one, so that linear motion consists of a rotation around this circle. One transformation to these “normalized coordinates” (x_N, x'_N) is given by

$$\begin{aligned} x(s) &= \sqrt{\beta(s)}x_N(s) , \\ x'(s) &= \frac{1}{\sqrt{\beta(s)}}x'_N(s) - \frac{\alpha(s)}{\sqrt{\beta(s)}}x_N(s) . \end{aligned} \quad (2.23)$$

Both x_N and x'_N have units of $m^{1/2}$ as do all distances in the normalized coordinate system. After this transformation both M_{12} and M become pure rotation matrices, rotating in the clockwise direction in the (x_N, x'_N) plane by angles of $\Delta\psi$ and $2\pi Q$ respectively. Both α and β are functions of the longitudinal coordinate s , but due to the periodicity of the lattice functions they are independent of t and thus so is the one-turn mapping.

Because linear phase space motion is nothing more than a rotation, if the rotation angle is a rational multiple of 2π (or the tune Q is rational), the particle returns to the same phase space position in some number of turns. A perturbation at a particular location in the accelerator having the same periodicity in the phase angle will always kick the particle in the same way, possibly creating amplitude growth, luminosity degradation and particle loss. Generalizing to both transverse dimensions, the resonance condition on the horizontal and vertical tunes is given by

$$jQ_x + kQ_y = l, \quad (2.24)$$

where j , k and l are integers. The perturbations mentioned above, periodic in the phase, drive these resonances — they are caused by nonlinear forces such as nonlinear magnet errors and magnetic forces felt by particles comprising colliding beams (the beam-beam force). Following (2.24), resonances have nonlinear kicks with a phase dependence $\cos(j\psi_x + k\psi_y)$.

2.3 GENERATING FUNCTIONS AND CANONICAL TRANSFORMATIONS

Hill's equation, Equation (2.7), is also the equation of motion for a harmonic oscillator with a time-dependent restoring force and no damping. A nonautonomous Hamiltonian can be written for such an oscillator:

$$H(x, p_x; s) = \frac{p_x^2}{2} + K(s)\frac{x^2}{2}, \quad (2.25)$$

where p_x is the canonical momentum associated with the position x . Application of Hamilton's equations immediately gives $p_x = x'$, so the coordinate x' is the canonical conjugate of the position x . This Hamiltonian can be canonically transformed to the form of an action-angle harmonic oscillator with the time-dependent type 1 generating function (Goldstein 1980, Chapter 9):

$$G_1([x, x'] \rightarrow [\psi, J]; s) = -\frac{x^2}{2\beta(s)} [\tan \psi(s) + \alpha(s)]. \quad (2.26)$$

This nontrivially produces the coordinate transformations and new Hamiltonian

$$\begin{aligned} x &= \sqrt{2J\beta} \cos \psi(s) , \\ x' &= -\sqrt{2J/\beta} [\sin \psi(s) + \alpha(s) \cos \psi(s)] , \\ H(\psi, J; s) &= H(x, x'; s) + \frac{dG_1}{ds} = \frac{J}{\beta(s)} . \end{aligned} \quad (2.27)$$

This is exactly the same as the harmonic solution, Equation (2.8), of Hill's equation mentioned previously, but this approach also identifies the appropriate canonical coordinates for a Hamiltonian analysis of the linear problem.

Motion will be expressed in a “discrete” Hamiltonian formalism throughout this thesis, where one-turn and N-turn maps similar to the linear map of Equation (2.20) are generated from the discrete Hamiltonian H and the corresponding discrete forms of Hamilton's equations:

$$\frac{\Delta x_N}{\Delta t} = \frac{\partial H}{\partial x'_N} , \quad \frac{\Delta x'_N}{\Delta t} = -\frac{\partial H}{\partial x_N} . \quad (2.28)$$

The linear one-turn motion over the ring is reproduced if the linear Hamiltonian (2.27) is integrated over one ring revolution. Then the discrete Hamiltonian and one-turn discrete equations of motion for the canonical coordinates (ψ, J) are:

$$\begin{aligned} H_1(\psi, J) &= 2\pi QJ , \\ \Delta\psi &= 2\pi Q , \\ \Delta J &= 0 . \end{aligned} \quad (2.29)$$

Since the beta function is periodic around the ring, the linear one-turn Hamiltonian H_1 is independent of turn number if the tune of the synchrotron is constant.

In order for the discrete forms of Hamilton's equation to retain their form when coordinate transformations are applied to the Hamiltonian, it is necessary and sufficient to require these transformations to be canonical. In this dissertation a variety of (possibly time-dependent) generating functions are used to generate these canonical transformations (Goldstein 1980, Landau and Lifshitz 1975).

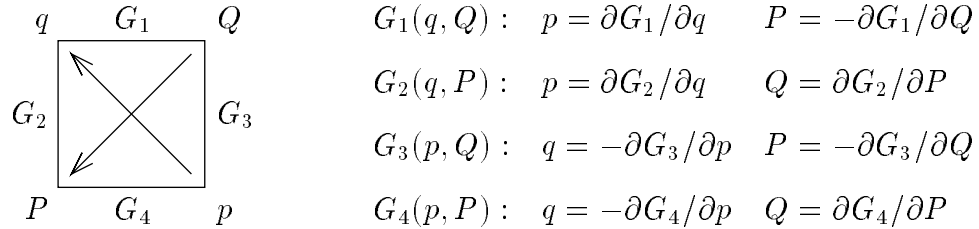


Figure 2.4: The generating function mnemonic square. The generating functions G_i are functions of the coordinates that bracket them, and partial derivatives in the direction of the arrows are positive. The Hamiltonian is also changed by an amount dG_i/dt in the transformation, if the generating function is time-dependent.

There are four common types of canonical transformations from coordinates (q, p) to (Q, P) , imaginatively named type 1 through type 4. For example, the type 1 generating function used above depends only on the old and new coordinates q and Q , not on the momenta p and P ; it gives the transformation equations

$$\begin{aligned}
 p &= \frac{\partial G_1(q, Q; t)}{\partial q}, \\
 P &= -\frac{\partial G_1(q, Q; t)}{\partial Q}, \\
 H(q, p; t) &\rightarrow H(Q, P; T) + \frac{dG_1(q, Q; t)}{dt}.
 \end{aligned} \tag{2.30}$$

The four types of generating functions and their respective transformation equations may be conveniently summarized using a mnemonic square similar to that used in thermodynamics, as shown in Figure (2.4). All linear transformations, time dependent or not, are canonical — when these are used the coordinate transformations will be stated for clarity. Other types of canonical transformations applied here are stated explicitly by their generating functions.

At several places in this thesis, discrete Hamiltonians are “integrated” (or, more properly, summed) to give equations of motion over timescales of N turns, where N is an integer. This requires rescaling the time coordinate; however the product of the Lagrange action and time used to derive Hamilton’s equations from a least-

action principle (Goldstein 1980, p. 364),

$$d\mathcal{L} \equiv [pq - H(p, q)]dt , \quad (2.31)$$

remains invariant under this transformation if the Hamiltonian is scaled to suit the time change. Since this is implicit in the summation process, the only change necessary for such a transformation to respect the difference forms of Hamilton's equations is the rescaling of the time coordinate, $t \rightarrow Nt \equiv T$.

2.4 LONGITUDINAL MOTION AND CHROMATICITY

In the context of the stability of transverse motion, longitudinal dynamics are important because they provide a mechanism for tune modulation to exist in every machine which uses RF systems to longitudinally stabilize and accelerate particle beams. The parameter used to quantify the coupling of the fractional momentum offset to the transverse tune in each plane is called the chromaticity ξ_i ; it is defined by

$$\Delta Q_i = \xi_i \delta \quad (2.32)$$

in each plane. Here $\delta \equiv \Delta p/p_0$ is the fractional momentum offset from the ideal design momentum p_0 . European convention differs significantly in definition of the chromaticity, using the fractional tune shift $\Delta Q/Q$ instead of ΔQ . Chromatic effects arise from the momentum dependence of the focusing strength of quadrupoles — if a particle has a larger energy than the design energy, it is focused less strongly and executes a smaller number of betatron oscillations in one machine revolution. For a simple uncorrected alternating-gradient synchrotron the chromaticity is roughly equal in magnitude and opposite in sign to the tune.

For most machines such a large net chromaticity is undesirable, as particles with even small fractional momentum offsets can experience tune shifts large enough to shift them onto undesirable resonances. Chromaticity is adjusted with the

addition of correction sextupoles at points of nonzero dispersion in each plane, since dispersion is the coupling between momentum offset and transverse position; for example, horizontal dispersion gives

$$x(\text{total}) = x(\text{closed orbit}) + \eta_x \frac{\Delta p}{p_0}. \quad (2.33)$$

Examining Equation (2.6) for a normal sextupole ($n = 2$) and including the effect of dispersion in the horizontal plane to first order in momentum offset, we find that sextupoles give kicks linear in displacement, or momentum-dependent quadrupole kicks:

$$\Delta x' - i\Delta y' = -\tilde{b}_2 \left[(x + iy)^2 + 2 \frac{\Delta p}{p} \eta_x (x + iy) \right]. \quad (2.34)$$

For maximum efficiency a normal chromaticity correction sextupole would be placed at a point with high horizontal dispersion. Using the tune shift from a quadrupole kick, Equation (2.22), one can immediately find the contribution to the total chromaticity from a distribution of normal sextupoles:

$$\begin{aligned} \xi_x &= \frac{1}{2\pi} \sum_i \eta_x(s_i) \beta_x(s_i) \tilde{b}_2(s_i), \\ \xi_y &= -\frac{1}{2\pi} \sum_i \eta_x(s_i) \beta_y(s_i) \tilde{b}_2(s_i). \end{aligned} \quad (2.35)$$

It is also important to note that though sextupoles can correct the chromaticity, they also introduce nonlinear kicks and transverse coupling.

Particles with momentum offsets subject to RF focusing also execute synchrotron oscillations, where δ is not constant but varies sinusoidally as though it were being modulated. Although investigation of the longitudinal phase space of a particle is complicated (Edwards and Syphers 1987, chapter 2), for longitudinal beam distributions much smaller than the RF bucket size it is a good approximation that all particles have their momentum offsets oscillating at the same frequency, the synchrotron frequency Q_s . In the absence of explicit tune

modulation (as was used in E778) and strong power supply ripple, this is the source of tune modulation that motivates the long-term stability inquiries raised in later chapters.